SUPPLEMENTARY INFORMATION

Supplementary Table 1. Alignment statistics for sequencing reads.

	HeLa mRNA-Seq, 32 h			HeLa Ribosome Profiling, 32 h			Neutrophil mRNA-Seq		Neut. Ribosome Profiling	
	Mock	miR-155	miR-1	Mock	miR-155	miR-1	WT	*mir-223*$^{-/Y}$	WT	*mir-223*$^{-/Y}$
Raw number of reads	11,441,416	14,392,817	13,505,056	18,029,685	17,454,122	17,643,682	17,303,502	16,280,254	16,418,487	18,072,590
Uniquely mapping reads										
To genome (first-phase)	5,722,434	7,447,242	7,179,753	8,533,140	8,975,586	8,902,916	8,362,287	7,806,247	10,239,553	11,080,166
To reference transcript database (second-phase)	403,577	499,784	487,120	758,639	753,094	704,680	593,777	584,578	788,191	869,904
Total mapping uniquely	6,126,011	7,947,026	7,666,873	9,291,779	9,728,680	9,607,596	8,956,064	8,390,825	11,027,744	11,950,070
Percentage of raw reads mapping uniquely	53.5	55.2	56.8	51.5	55.7	54.5	51.8	51.5	67.2	66.1
rRNA unique matches	748,043	968,296	803,583	3,114,740	3,641,076	3,792,787	365,308	439,258	4,633,841	4,831,036
Percentage rRNA unique matches	12.2	12.2	10.5	33.5	37.4	39.5	4.1	5.2	42.0	40.4
Unambiguous, unique gene-mapping reads										
Total mapped reads (library size)	4,606,993	6,019,691	5,910,777	5,439,248	5,342,830	5,102,548	7,652,330	7,070,727	6,002,118	6,688,548
Percentage of all unique matches	75.2	75.8	77.1	58.5	54.9	53.1	85.4	84.3	54.4	56.0
Number of reads mapping to exons	4,095,694	5,353,615	5,249,653	5,379,200	5,279,217	5,037,521	6,542,225	6,162,103	5,945,873	6,627,659
Number of reads mapping to coding exons	2,762,359	3,612,248	3,493,711	5,136,392	5,011,176	4,784,714	4,500,718	4,275,842	5,562,427	6,200,226
Number of reads mapping to introns	511,299	666,076	661,124	60,048	63,613	65,027	1,110,105	908,624	56,245	60,889
Percentage coding exon reads, out of all reads mapping to exons	67.5	67.5	66.6	95.5	94.9	95.0	68.8	69.4	93.6	93.6

Supplementary Table 2. Alignment statistics for sequencing reads, for samples collected at 12 h post-transfection.

	HeLa mRNA-Seq, 12 h			HeLa Ribosome Profiling, 12 h		
	Mock	miR-155	miR-1	Mock	miR-155	miR-1
Raw number of reads	21,623,454	21,388,074	21,681,406	16,793,006	16,792,228	15,741,337
Uniquely mapping reads						
To genome (first-phase)	10,743,704	11,232,931	11,957,592	7,882,398	7,923,788	6,669,746
To reference transcript database (second-phase)	708,950	753,144	771,463	722,046	912,444	693,775
Total mapping uniquely	11,452,654	11,986,075	12,729,055	8,604,444	8,836,232	7,363,521
Percentage of raw reads mapping uniquely	53.0	56.0	58.7	51.2	52.6	46.8
rRNA unique matches	1,172,686	1,326,092	1,375,560	2,984,080	1,802,419	1,851,953
Percentage rRNA unique matches	10.9	11.8	11.5	37.9	22.7	27.8
Unambiguous, unique gene-mapping reads						
Total mapped reads (library size)	8,746,696	9,147,411	9,706,156	4,999,224	6,296,140	4,927,498
Percentage of all unique matches	76.4	76.3	76.3	58.1	71.3	66.9
Number of reads mapping to exons	7,524,106	8,018,834	8,362,731	4,940,460	6,217,253	4,864,783
Number of reads mapping to coding exons	4,882,314	5,340,751	5,544,369	4,712,453	5,908,841	4,590,167
Number of reads mapping to introns	1,222,590	1,128,577	1,343,425	58,764	78,887	62,715
Percentage coding exon reads, out of all reads mapping to exons	64.9	66.6	66.3	95.4	95.0	94.4

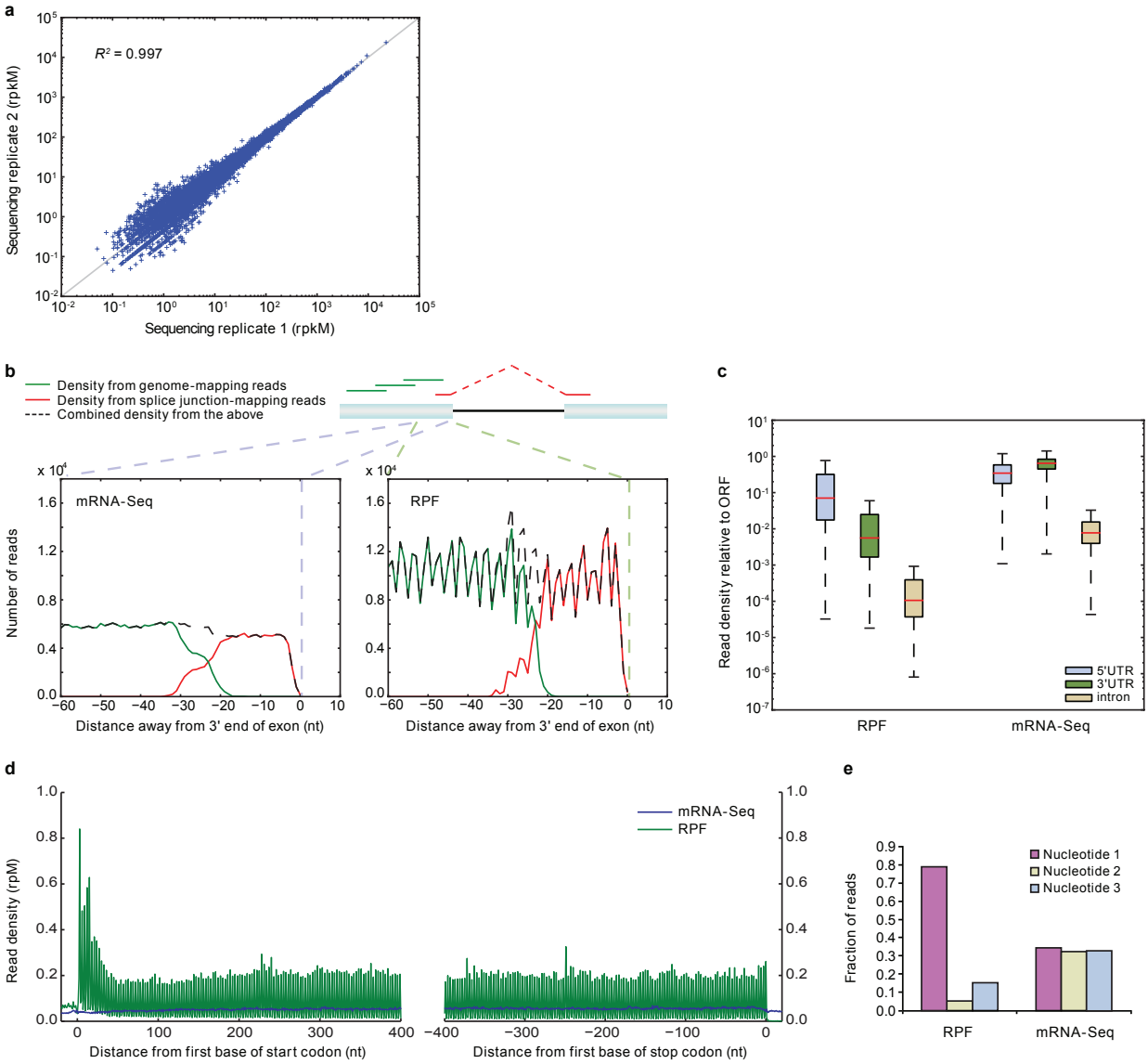

Supplementary Figure 1. Ribosome profiling in mammalian cells captured features of translation. **a**, Correspondence between gene expression quantified in two different sequencing replicates of the same library. Expression values are in terms of reads per million reads mapped to genes per kilobase coding exon model (rpkM). The R^2 derived from Pearson's correlation is indicated. **b**, Density of mRNA-Seq tags and RPFs near the 3' ends of exons, which indicates that splice isoforms used in our reference transcript database were representative of the transcriptome. Plotted are 5' termini of mRNA-Seq tags (*left*) or RPFs (*right*), for genome-mapping reads (green solid line), splice junction-mapping reads (red solid line) and the combined read density (black dashed line). Composite data are shown for all exons ≥100 nucleotides (nt) in length. Athough reads coming from the rest of the exon can map to the genome irrespective of which splice isoforms were expressed, reads spanning the splice junctions might not have sufficient length on the 5' side of the junction, to be confidently mapped by the mapping program. Hence, if a gene were expressed in multiple isoforms in the cell or if we picked the wrong isoform, reads coming from the 3' ends of certain exons of the correct isoforms might not be mapped. This was, however, not a major problem as the read density obtained for this region overall was >90% that of the rest of the exon. The jagged pattern observed in the plot for RPFs was explained by most exons being in the same reading frame (together with the codon nucleotide preference observed with ribosome profiling, e.g., Fig. 1d and Supplementary Fig. 1e) **c**, Expression levels from different regions of mRNAs, quantified by RPFs and mRNA-Seq tags. Expression values from each indicated region in a transcript was normalized to that in the associated ORF and plotted as relative density, as quantified by RPFs and mRNA-Seq tags. **d**, Density of RPFs and mRNA-Seq tags near the beginnings and ends of ORFs in mouse neutrophils. RPF and mRNA-Seq density are plotted as in Fig. 1c. Composite data are shown for ≥ 600-nucleotide ORFs that passed our threshold for quantification (≥100 RPFs and ≥100 mRNA-Seq tags). **e**, Fraction of RPFs and mRNA-Seq tags mapping to each of the three codon nucleotides in panel **d**. Our samples exhibited small differences in the ratio of reads mapping to codon nucleotides 3 and 1, which we attribute to the extent of RNase I digestion, with more reads at codon nucleotide 3 correlated with less thorough digestion (as evaluated on sucrose gradient profiles). Our mouse neutrophil samples were more extensively digested than were the HeLa samples, and the reads exhibited an even stronger (80%) preference for codon nucleotide 1.

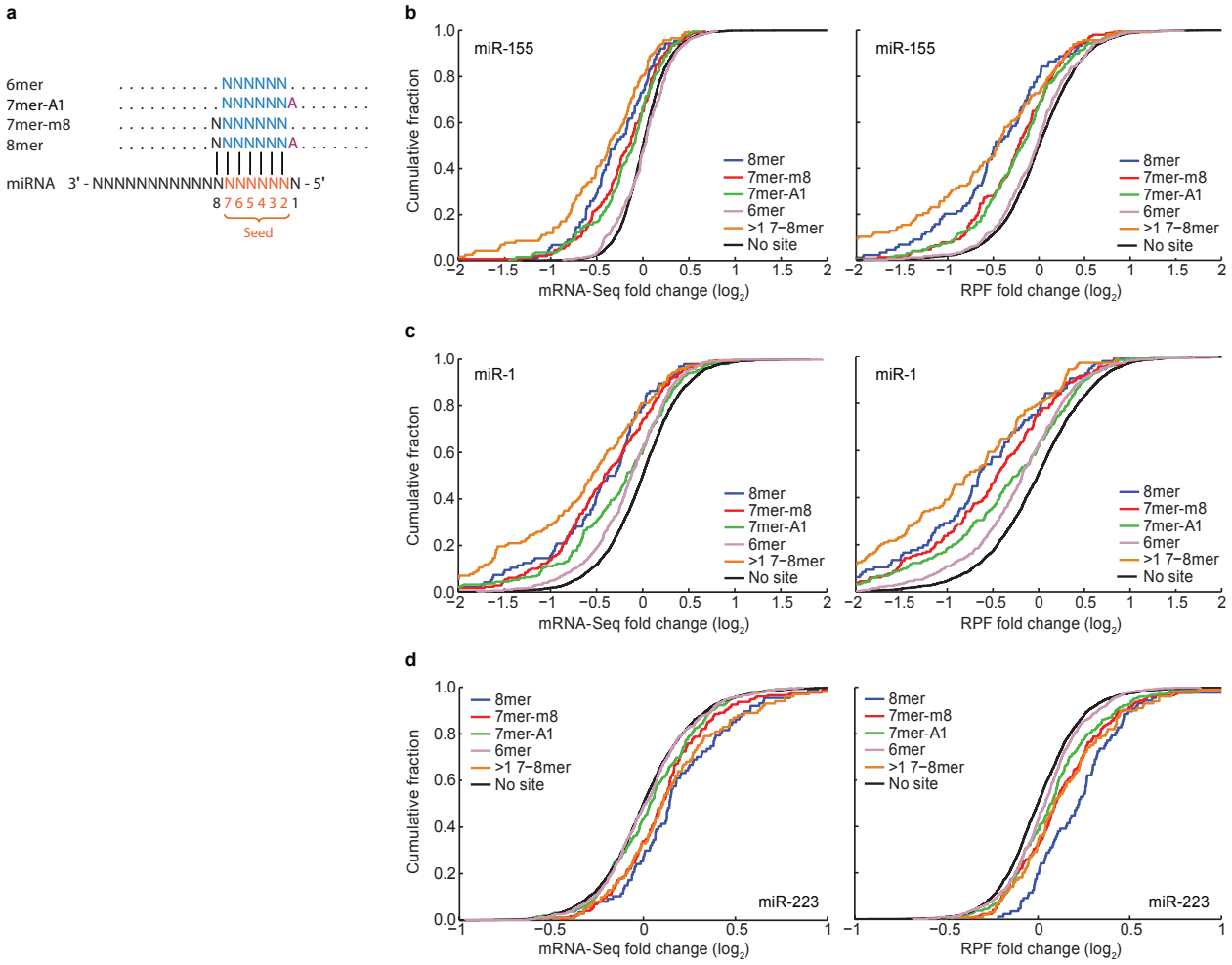

Supplementary Figure 2. Analyses of miRNA-dependent changes, which showed that ribosome profiling, like mRNA profiling, captured the characteristic hierarchy of site efficacies. **a**, Different types of seed-matched sites[2]. **b**, Cumulative distributions of mRNA-Seq changes (*left*) and RPF changes (*right*) after introducing miR-155. Plotted are distributions for genes with either a single 3'UTR site of the indicated type, multiple 7–8mer 3'UTR sites, or no site. Only genes that passed our threshold for quantification (≥100 RPFs and ≥100 mRNA-Seq tags) were considered. **c**, Cumulative distributions of mRNA-Seq changes (*left*) and RPF changes (*right*) after introducing miR-1. Otherwise, as in panel **b**. **d**, Cumulative distributions of mRNA-Seq changes (*left*) and RPF changes (*right*) after deleting *mir-223*. Otherwise, as in panel **b**.

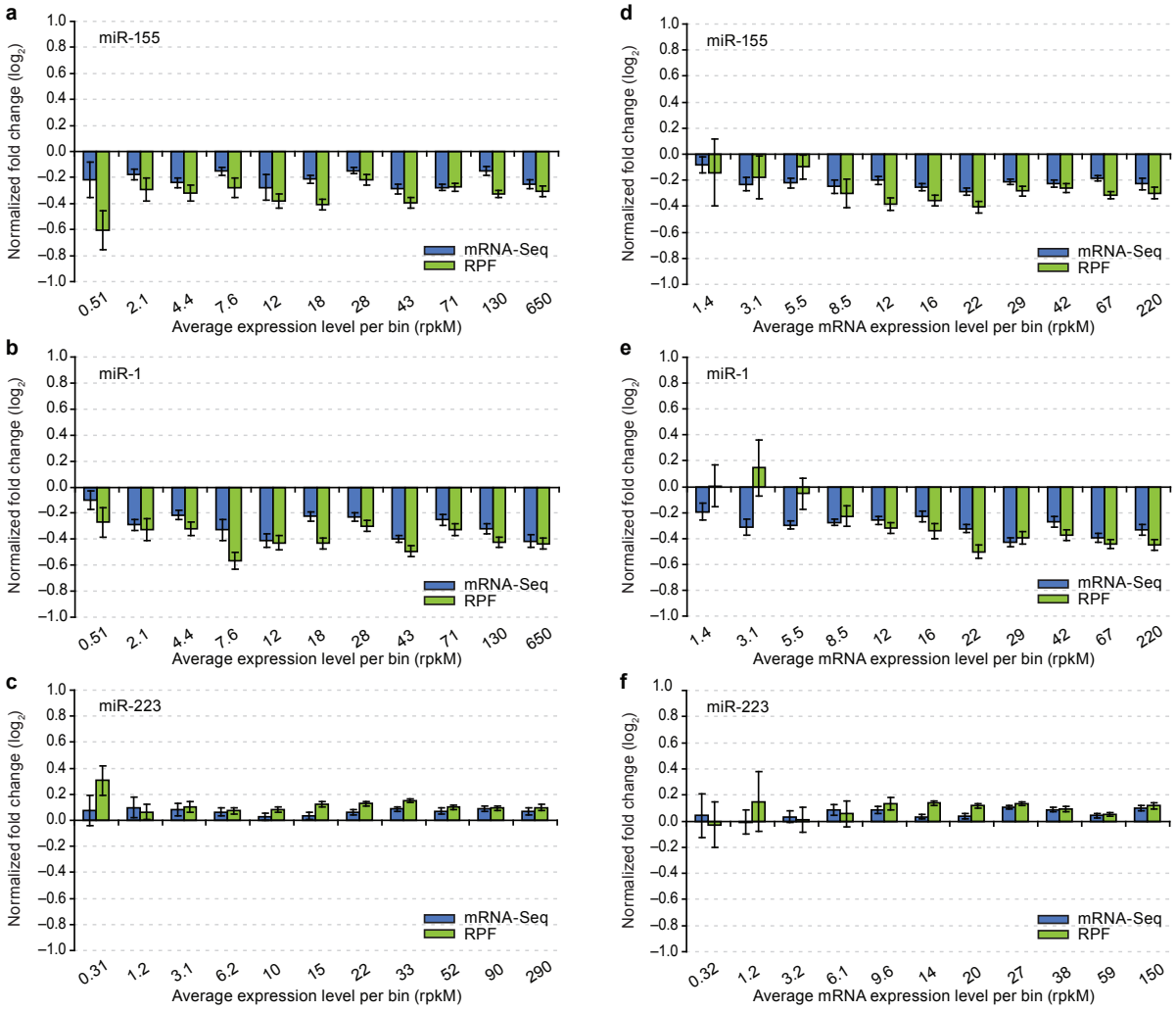

Supplementary Figure 3. MicroRNA targets expressed at different levels were similarly repressed. **a**, Changes in RPFs and mRNA-Seq tags from mRNAs with cognate sites, after introducing miR-155 into HeLa cells. Genes were binned in groups of 1000 based on expression, as measured by RPF density in mock-transfected cells. The average RPF expression density for each bin is indicated in terms of reads per million reads mapped to genes per kilobase coding exon model (rpkM). Plotted for each bin are the normalized aggregate fold changes in RPFs (green) and mRNA-Seq tags (blue). In each case, the normalized aggregate fold change was derived by dividing the aggregate fold change for genes with 3'UTR sites by that for genes without sites anywhere in their mRNA. To estimate the average aggregate fold change value for genes without sites, 100 control cohorts were generated by randomly selecting genes without sites to replace genes with sites. The mean fold change for these 100 cohorts was then used for normalization in each bin. Error bars represent the standard deviations of each of these 100 cohorts. **b**, As in panel **a**, but plotting repression of mRNAs with miR-1 3'UTR sites after introducing miR-1. **c**, As in panel **a**, but plotting derepression of mRNAs with miR-223 3'UTR sites, comparing samples from neutrophils derived from *mir-223* knockout mice to those from neutrophils derived from wild-type mice. Genes were binned according to their expression levels in the KO dataset. The top 80 most highly expressed genes were excluded from this analysis because their high expression levels (otherwise comprising >60% of the total RPFs in the last bin) led to high variability for the control cohorts of the last bin. **d**, As in panel **a**, but genes were binned in groups of 1000 based on expression as measured by mRNA-Seq density (rpkM) rather than RPF density. **e**, As in panel **b**, but genes were binned in groups of 1000 based on expression as measured by mRNA-Seq density (rpkM). **f**, As in panel **c**, but genes were binned in groups of 1000 based on expression as measured by mRNA-Seq density (rpkM). The top 80 most highly expressed genes were again excluded from the analysis (otherwise comprising >56% of the total mRNA-Seq tags in the last bin).

To examine a potential relationship between gene expression and miRNA-mediated repression, genes were grouped by expression level, and then for each bin the results for messages with at least one 3'UTR site were compared to those without a site anywhere in the mRNA. For example, in the miR-155 experiment, genes with uniquely mapping RPFs were assigned to bins, with 1000 distinct genes per bin, based on the density of RPFs in mock-transfected HeLa cells (panel **a**). Because genes in each bin were analyzed in aggregate, a read threshold for individual genes was not required, allowing inclusion of data from 11,000 distinct genes, which ranged broadly in expression (more than 1000-fold difference between the first and last bins). Except for one outlier bin, messages with miR-155 sites underwent repression of similar magnitude regardless of their expression level (panel **a**). The same was true in the miR-1 experiment (panel **b**). When we examined endogenous miRNA:target interactions, as detected by monitoring derepression ($\log_2$-fold increases rather than decreases) in *mir-223* KO cells, analogous results were obtained (panel **c**). Although the RPF change for the bin with the lowest-expressed genes appeared greater than that for other bins in the miR-155 and miR-223 experiments, this change was accompanied by larger variability (note error bars) and was not observed in neighboring bins, nor when the analysis was repeated using mRNA-Seq tags to group the genes based on mRNA expression (panels **d**–**f**). Moreover, in the miR-1 experiment the RPF change for this bin was no greater than that for other bins (panel **b**), further supporting the conclusion that miRNAs do not repress their lowly expressed targets more potently than they do their moderately expressed targets.

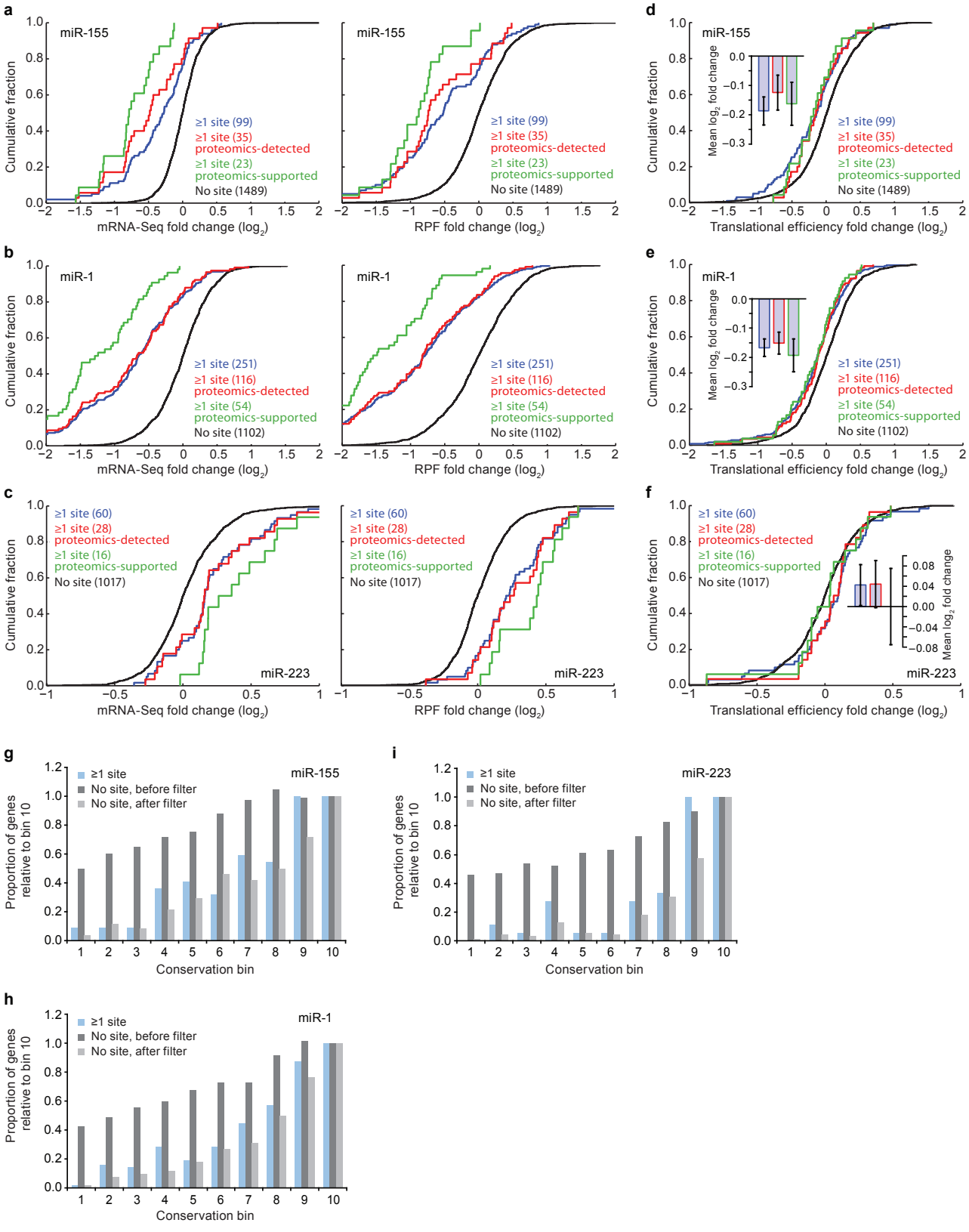

Supplementary Figure 4. MicroRNA targets with conserved 3'UTR sites were repressed mostly through mRNA destabilization. **a**, Cumulative distributions of mRNA-Seq changes (*left*) and RPF changes (*right*) after introducing miR-155, for genes with conserved sites to miR-155. Plotted are distributions for the genes with ≥1 miR-155 conserved 3'UTR site (blue), the subset of these genes detected in the pSILAC experiment (proteomics-detected, red), the subset of the proteomics-detected genes with proteins responding with $\log_2$-fold change ≤ –0.3 (proteomics-supported, green), and similarly-conserved control genes, which lacked miR-155 sites throughout their mRNAs (no site, black). The number of genes in each category is indicated in parentheses. Only genes that passed our expression thresholds (≥100 RPFs and ≥100 mRNA-Seq tags) were considered. Note that the "no site" distribution comprised genes selected such that their 3'UTRs were conserved at similar levels as the 3'UTRs with conserved sites (discussed below), hence the smaller number of genes compared to the "no site" distribution in Fig. 2a. **b**, Cumulative distributions of

mRNA-Seq changes (*left*) and RPF changes (*right*) after introducing miR-1. Otherwise, as in panel **a**. **c**, Cumulative distributions of mRNA-Seq changes (*left*) and RPF changes (*right)* after deleting *mir-223*. Otherwise, as in panel **a**, with proteomics-supported genes referring to genes with proteins that responded with $\log_2$-fold change ≥ 0.3 in the SILAC experiment. **d**, Cumulative distributions of translational efficiency changes for the polyadenylated mRNA that remained after introducing miR-155. For each gene, the translational efficiency change was calculated by normalizing the RPF change by the mRNA-Seq change. The cumulative distributions of translational efficiency changes were then plotted, as in panel **a**. For each distribution, the mean $\log_2$-fold change (± standard error) is shown in the inset. **e**, Cumulative distributions of translational efficiency changes for the polyadenylated mRNA that remained after introducing miR-1. Otherwise, as in panel **d**. **f**, Cumulative distributions of translational efficiency changes for the polyadenylated mRNA that remained after deleting *mir-223*. Otherwise, as in panel **d**. **g**, Distribution of quantified genes in the miR-155 experiment across different conservation bins. Quantified genes with conserved sites to miR-155 (blue bars) are represented in terms of their proportion across the different conservation bins[1], with the fraction in bin 10 (most highly conserved) set to 1.0. Similarly, the proportions of quantified genes without sites are shown before (dark grey bars) and after (light grey bars) controlling for conservation levels, as described in the following paragraph. Genes in the latter group made up the "no site" distribution plotted in panels **a** and **d**. **h**, Distribution of quantified genes in the miR-1 experiment across different conservation bins. Otherwise, as in panel **g**. **i**, Distribution of quantified genes in the miR-223 experiment across different conservation bins. Otherwise, as in panel **g**.

Due to concern that 3'UTRs with conserved sites were expected to be more conserved than those without sites, which might influence our analyses of conserved targets, we controlled for conservation levels using data from Friedman et al. (2009), who divide genes into 10 bins based on 3'UTR conservation levels. We first determined the number of genes with sites in each of these bins. Then genes without sites were sampled from each bin until the population of genes without sites reached the same proportions across the different bins as the population of genes with sites. With this filter, genes that formed the "no site" distribution had 3'UTR conservation levels matching that of the conserved targets. For all three experiments, controlling for 3'UTR conservation did not significantly change the cumulative distribution plots for the no-site subsets of genes ($P > 0.24$, K–S test).

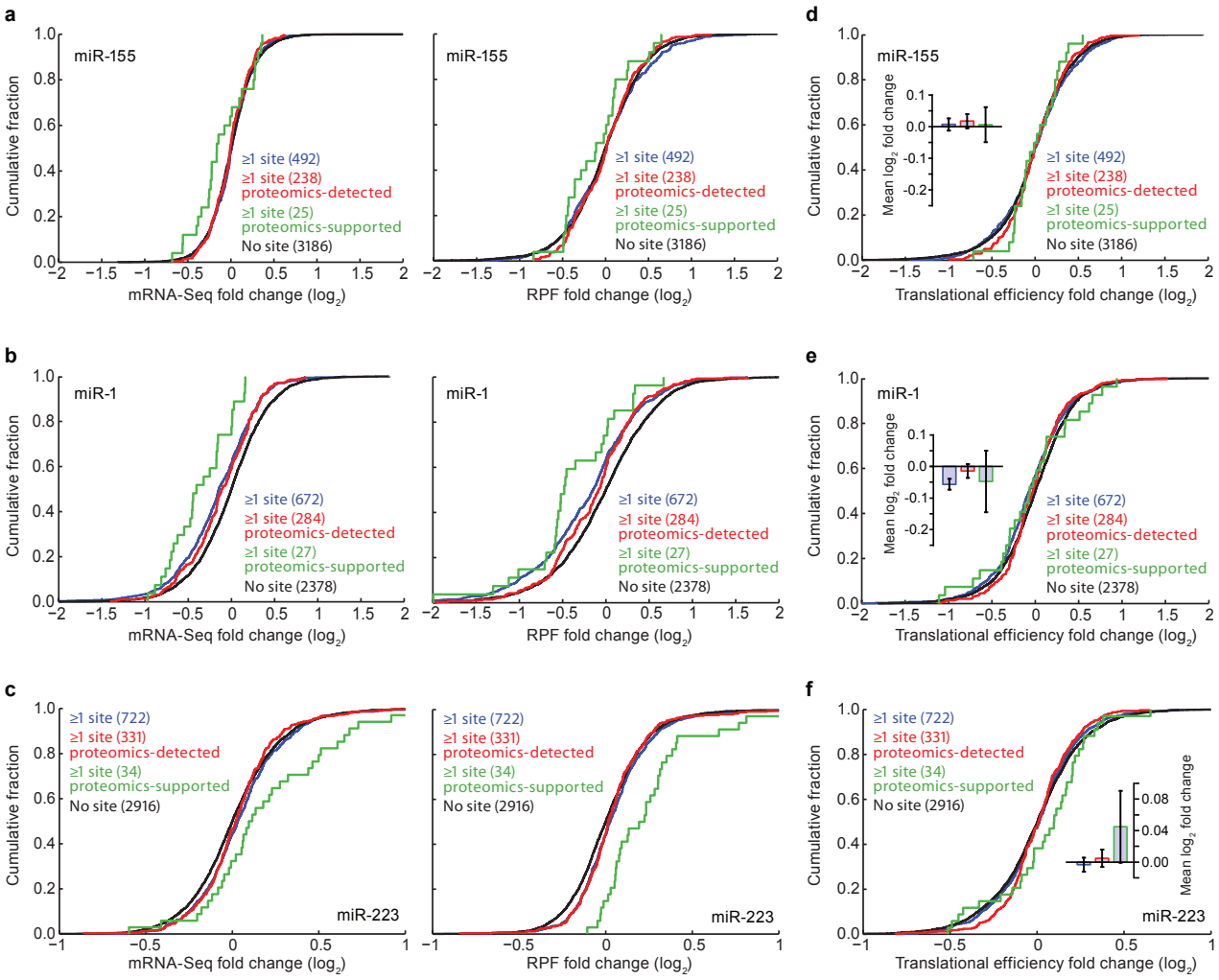

Supplementary Figure 5. MicroRNA targets with sites only in their ORFs were weakly repressed, mostly through mRNA destabilization. **a**, Cumulative distributions of mRNA-Seq changes (*left*) and RPF changes (*right*) after introducing miR-155. Plotted are distributions for the genes with ≥1 miR-155 ORF site (blue), the subset of these genes detected in the pSILAC experiment (proteomics-detected, red), the subset of the proteomics-detected genes with proteins responding with $\log_2$-fold change ≤ –0.3 (proteomics-supported, green), and the control genes, which lacked miR-155 sites throughout their mRNAs (no site, black). The number of genes in each category is indicated in parentheses. Only genes that passed our expression thresholds (≥100 RPFs and ≥100 mRNA-Seq tags) were considered, and genes with a miR-155 3'UTR site (6-nt seed match) were excluded. **b**, Cumulative distributions of mRNA-Seq changes (*left*) and RPF changes (*right*) after introducing miR-1. Otherwise, as in panel **a**. **c**, Cumulative distributions of mRNA-Seq changes (*left*) and RPF changes (*right*) after deleting *mir-223*. Otherwise, as in panel **a**, with proteomics-supported genes referring to genes with proteins that responded with $\log_2$-fold change ≥ 0.3 in the SILAC experiment. **d**, Cumulative distributions of translational efficiency changes for the polyadenylated mRNA that remained after introducing miR-155. For each gene, the translational efficiency change was calculated by normalizing the RPF change by the mRNA-Seq change. The cumulative distributions of translational efficiency changes were then plotted, as in panel **a**. For each distribution, the mean $\log_2$-fold change (± standard error) is shown in the inset. **e**, Cumulative distributions of translational efficiency changes for the polyadenylated mRNA that remained after introducing miR-1. Otherwise, as in panel **d**. **f**, Cumulative distributions of translational efficiency changes for the polyadenylated mRNA that remained after deleting *mir-223*. Otherwise, as in panel **d**.

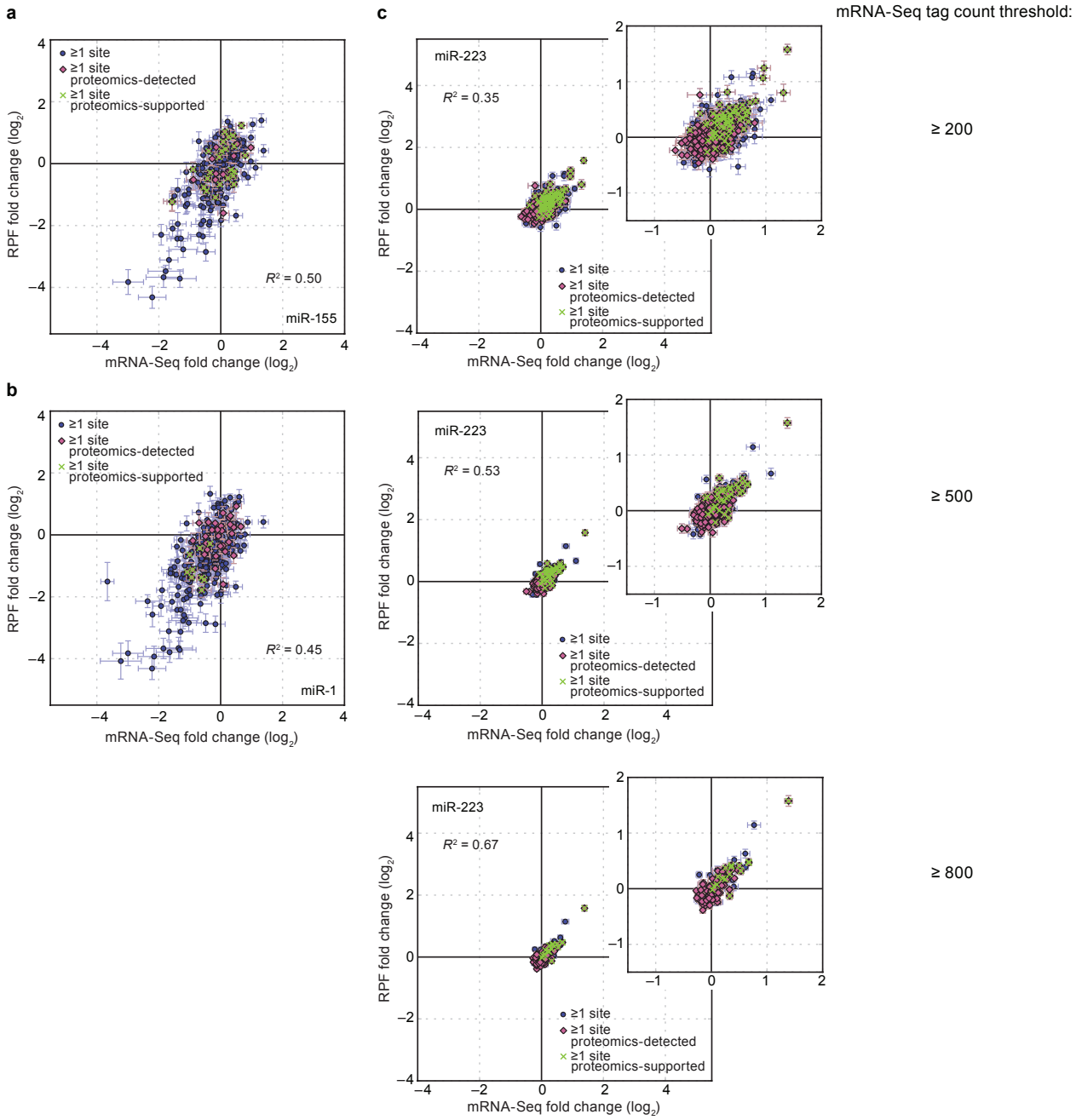

Supplementary Figure 6. Correspondence between ribosome changes and mRNA changes from miRNA targeting when using alternative quantification thresholds. **a**, Correspondence between ribosome (RPF) and mRNA (mRNA-Seq) changes after introducing miR-155, for genes that were only considered after relaxing the quantification thresholds from ≥100 reads each in the mRNA-Seq and RPF libraries (mock transfection) to ≥44 mRNA-Seq tags and ≥80 RPF reads (blue circles). Proteomics-detected targets and proteomics-supported targets are highlighted (pink diamonds and green crosses, respectively). Expected standard deviations (error bars) were calculated based on the number of reads obtained per gene and assuming random counting statistics. The R^2 derived from Pearson's correlation of all data is indicated. **b**, Correspondence between ribosome and mRNA changes after introducing miR-1, for genes that were only considered after relaxing the quantification thresholds from ≥100 reads each in the mRNA-Seq and RPF libraries (mock transfection) to ≥44 mRNA-Seq tags and ≥80 RPF reads. Otherwise, as in panel **a**. **c**, Correspondence between ribosome and mRNA changes after deleting *mir-223*, for genes considered at increasing stringency of mRNA-Seq quantification thresholds. The RPF read threshold was kept constant at ≥100 reads in the KO sample, while the threshold for the mRNA-Seq KO library was increased from ≥100 reads in Fig. 3e to ≥200 reads, ≥500 reads and ≥800 reads. Otherwise, as in panel **a**. Insets provide closer views of the corresponding sets of data.

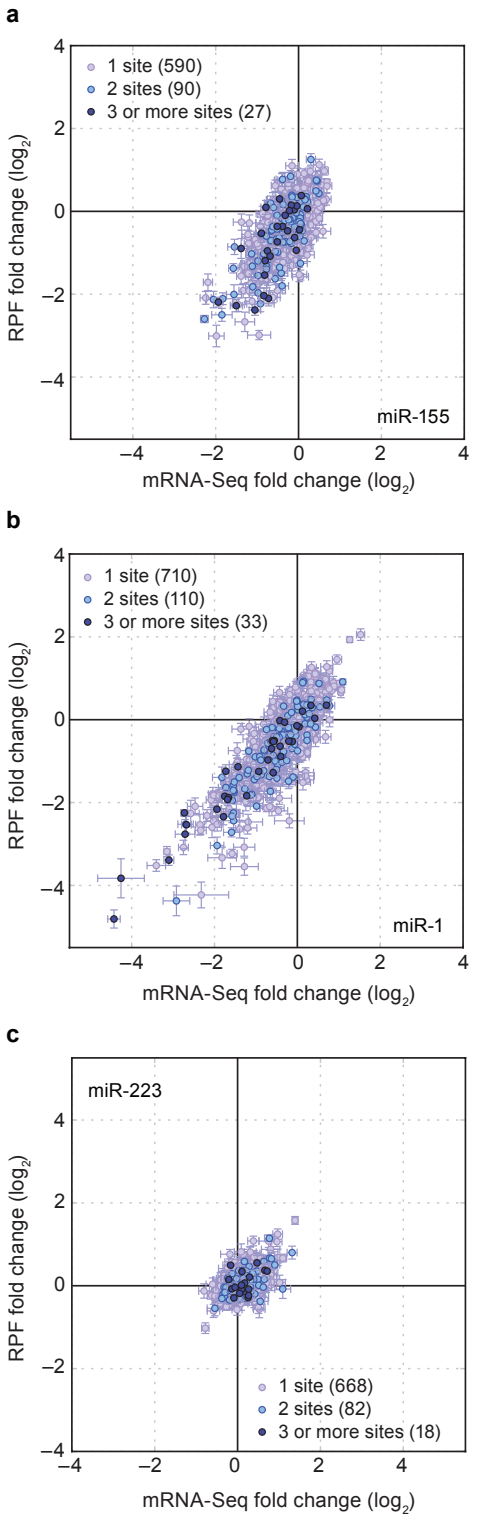

Supplementary Figure 7. Genes with multiple sites to the cognate miRNA were repressed in a manner similar to that of genes with single sites. **a**, Correspondence between ribosome (RPF) and mRNA (mRNA-Seq) changes after introducing miR-155, plotting data for the 707 quantified genes with at least one miR-155 3'UTR site. Genes with two sites and genes with at least three sites are highlighted (light blue circles and dark blue circles, respectively). Expected standard deviations (error bars) were calculated based on the number of reads obtained per gene and assuming random counting statistics. **b**, Correspondence between ribosome and mRNA changes after introducing miR-1, plotting data for the 853 quantified genes with at least one miR-1 3'UTR site. Otherwise, as in panel **a**. **c**, Correspondence between ribosome and mRNA changes after deleting *mir-223*, plotting data for the 768 quantified genes with at least one miR-223 3'UTR site. Otherwise, as in panel **a**.

Linear regression lines for each category of genes were calculated and tested against each other to see whether genes with different number of 3'UTR sites to the cognate miRNA responded differently. Of these comparisons, only two yielded statistically significant differences. In the miR-155 experiment, the regression slope of the genes with one site was different from that of the genes with two sites [$P = 0.04$, two-tailed Analysis of Covariance (ANCOVA) test]. In the miR-1 experiment, the regression slope of the genes with two sites was different from that of the genes with at least 3 sites ($P = 0.02$), but the difference in slope was in the opposite direction as observed for the greater number of sites in the miR-155 experiment. Because a consistent difference was not observed in any two datasets, we conclude that genes with multiple 3'UTR sites to the cognate miRNA were repressed in a manner similar to that of genes with single sites, i.e., mostly through mRNA destabilization.

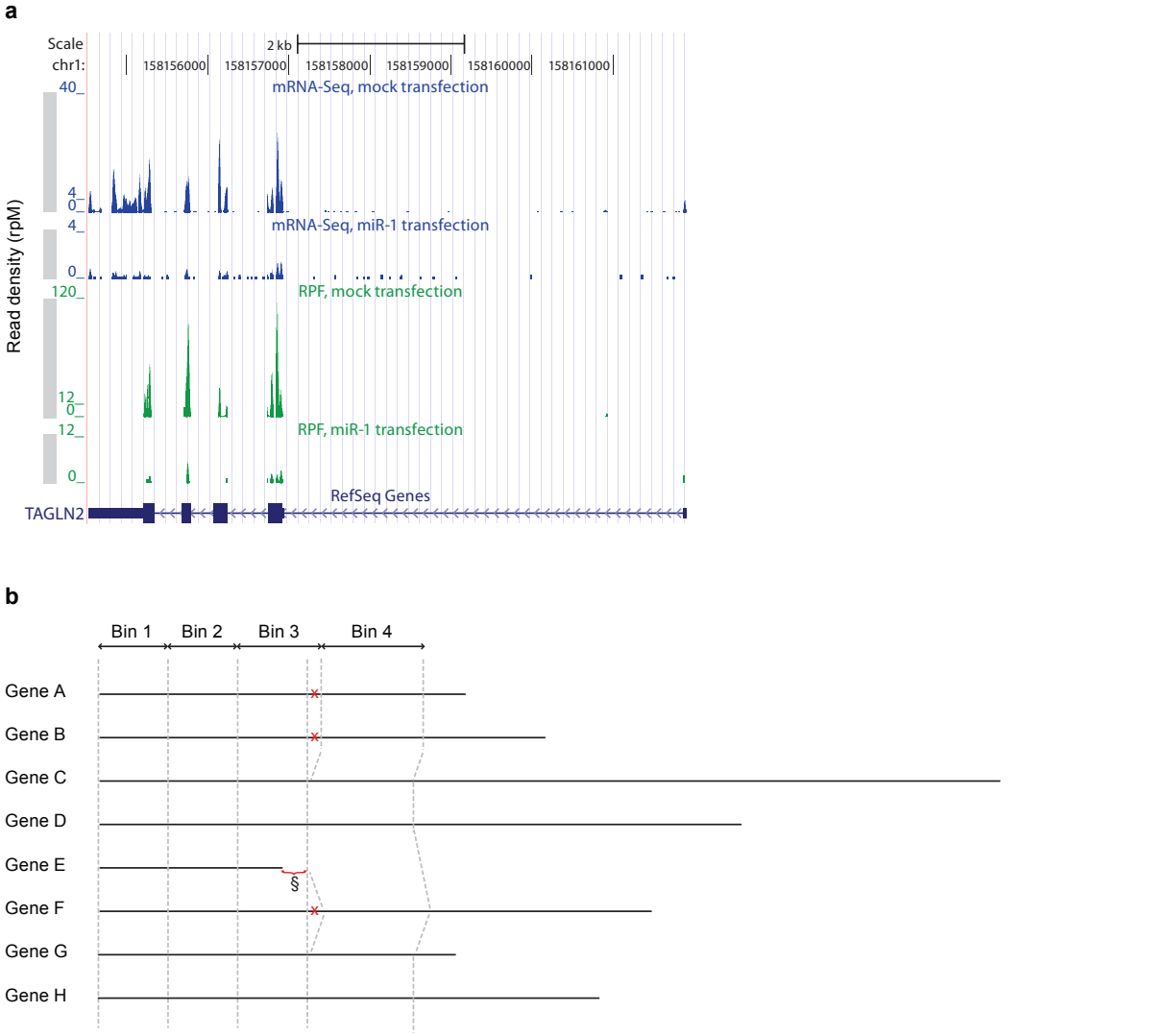

Supplementary Figure 8. Probing repression along the length of the mRNA. **a**, Read density from a gene with high sequence coverage. Normalized read density (mRNA-Seq, blue and RPF, green) for *TAGLN2*, a miR-1 target, is shown for the mock and miR-1 transfections. Note the ten-fold difference in the range of the y-axes between the coverage plots for the mock and miR-1 transfections. **b**, Schematic diagram of the binning strategy used in Fig. 4. All open reading frames within each category were lined up from the first nucleotide. All bases available were then assigned into 20 bins by drawing the same number of bases from each gene, for each bin. If a shortfall of bases resulted from reaching the ends of shorter genes (e.g., a shortfall of 3 nucleotides in Bin 3), the shortfall was alleviated by extending randomly selected representatives of the remaining genes (red x). The formation of subsequent bins then started from the remaining unassigned bases, as illustrated by the shifted frame. Later bins received a higher contribution from each remaining gene (as illustrated by the increased width in Bin 4), because a smaller number of genes remained after all bases in the shorter genes (represented by Gene E) had been assigned. This explains why the median bases plotted on the x-axes in Fig. 4 become further apart with increasing distance into the composite ORF. With this approach, every bin has the same number of nucleotides assigned to it (except the very last bin, which was discarded) and each successive bin represents a distance further away from the start of the composite ORF. To prevent spurious changes of just a few genes from dominating, bins were discarded if their read contribution derived from fewer than 20 genes. Because the number of genes with sites is smaller than that without sites, the 20-gene limit came at an earlier bin for the genes with sites, which explains why in Fig. 4 the plot for genes with sites has fewer bins than that for genes without sites.

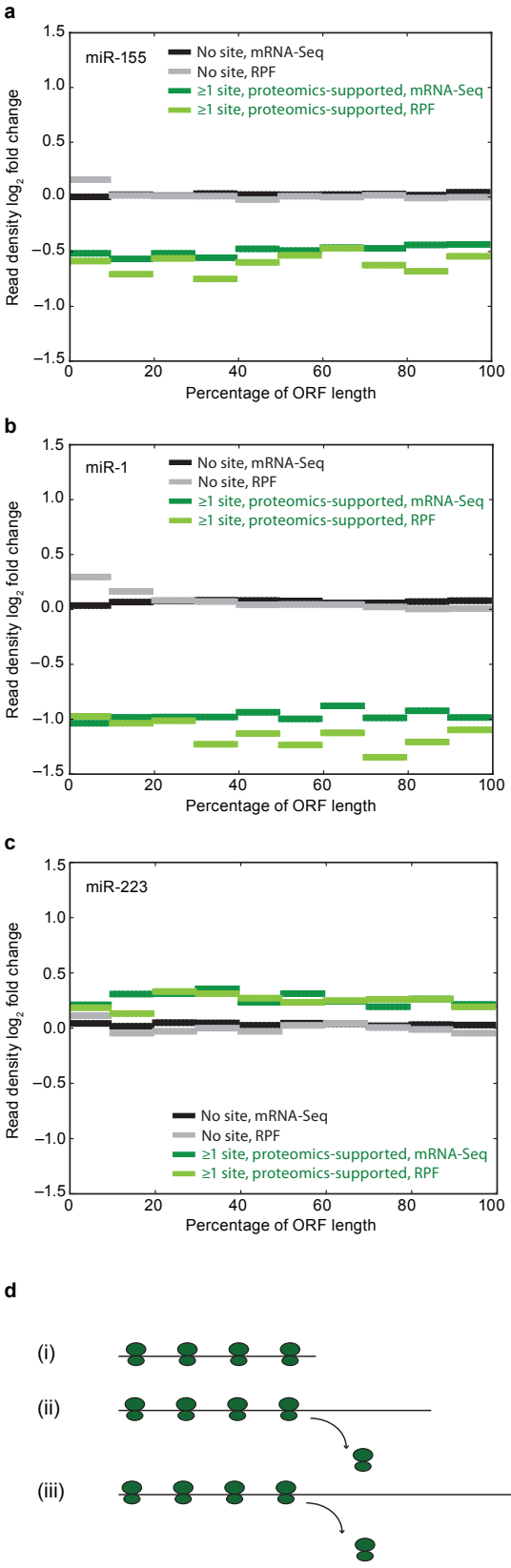

Supplementary Figure 9. Ribosome and mRNA changes were uniform along the percentage length of the ORFs. **a**, Ribosome and mRNA changes along the percentage length of the ORFs after introducing miR-155. The ORF of each quantified gene was divided into ten bins based on ORF length. Fold changes in RPFs and mRNA-Seq tags mapping to each bin were then plotted. Changes in RPFs and mRNA-Seq tags for mRNAs with no site (grey and black, respectively) and for proteomic-supported targets (light and dark green, respectively) are shown. **b**, Ribosome and mRNA changes along the percentage length of the ORFs after introducing miR-1. Otherwise, as in panel **a**. **c**, Ribosome and mRNA changes along the percentage length of the ORFs after deleting *mir-223*. Otherwise, as in panel **a**. **d**, Schematic diagram illustrating how a percentage-based measure could obscure drop-off effects. In this scenario, ribosomes start to drop off after traversing a certain length of the ORF. Based on the different lengths of the different ORFs, a drop-off at a similar absolute distance would occur at different percentage ORF lengths. In the extreme case of very short genes (i), no drop-off would occur and the lack of change at the ends of these ORFs could thereby obscure the drop-off effect from longer genes.

Due to the caveat presented in panel **d**, we adopted the alternative binning strategy used in Fig. 4, which makes use of a distance-based measure (Supplementary Fig. 8b). We note that for the miR-1 experiment, the percentage-based plot could suggest drop-off (panel **b**). However, if this were indeed the mechanism, this effect should become more obvious in the distance-based plot (Fig. 4b). The apparent incongruence of the two plots for the miR-1 experiment could be due to a few short genes with fewer reads towards the 3' ends of their ORFs having high sequence coverage and thus dominating changes in the percentage-based plot. The distance-based plot would not be confounded by this effect because shorter genes can only contribute to the early bins. To prevent the reciprocal effect of longer genes dominating the later bins and thus biasing the distance-based plots, we only plotted the bins which had read contribution from at least 20 genes in Fig. 4. Thus, for us to observe a drop-off effect in the distance-based plots, ribosome drop-off must be a mechanism that is sufficiently general to affect more than a few genes and genes of different length ranges. Because we do not see this effect, we conclude that for most targets ribosome drop-off is likely not a major component of the repression mechanism.

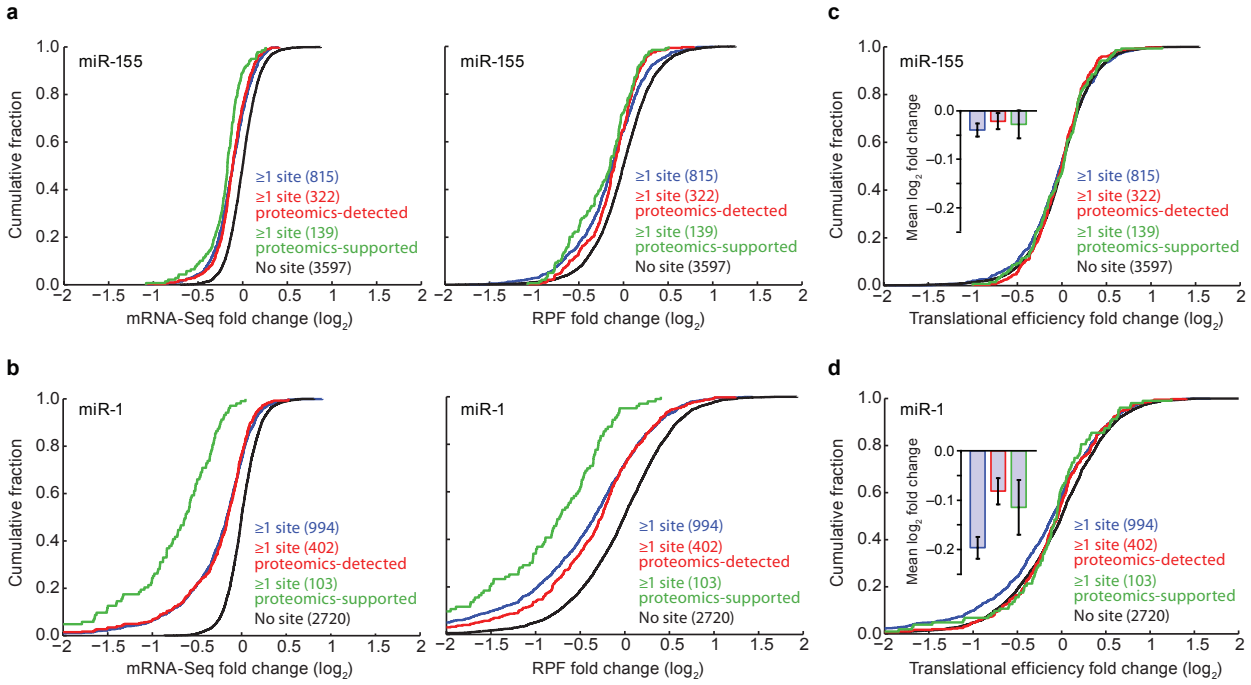

Supplementary Figure 10. At an earlier time point post-transfection most of the downregulation mediated by miRNAs was mostly through mRNA destabilization. **a**, Cumulative distributions of mRNA-Seq changes (*left*) and RPF changes (*right*) after introducing miR-155. Plotted are distributions for the genes with ≥1 miR-155 3'UTR site (blue), the subset of these genes detected in the pSILAC experiment (proteomics-detected, red), the subset of the proteomics-detected genes with proteins responding with $\log_2$-fold change ≤ –0.3 (proteomics-supported, green), and the control genes, which lacked miR-155 sites throughout their mRNAs (no site, black). The number of genes in each category is indicated in parentheses. Only genes that passed our expression thresholds (≥100 RPFs and ≥100 mRNA-Seq tags) were considered. **b**, Cumulative distributions of mRNA-Seq changes (*left*) and RPF changes (*right*) after introducing miR-1. Otherwise, as in panel **a**. **c**, Cumulative distributions of translational efficiency changes for the polyadenylated mRNA that remained after introducing miR-155. For each gene, the translational efficiency change was calculated by normalizing the RPF change by the mRNA-Seq change. The cumulative distributions of translational efficiency changes were then plotted, as in panel **a**. For each distribution, the mean $\log_2$-fold change (± standard error) is shown in the inset. **d**, Cumulative distributions of translational efficiency changes for the polyadenylated mRNA that remained after introducing miR-1. Otherwise, as in panel **c**.

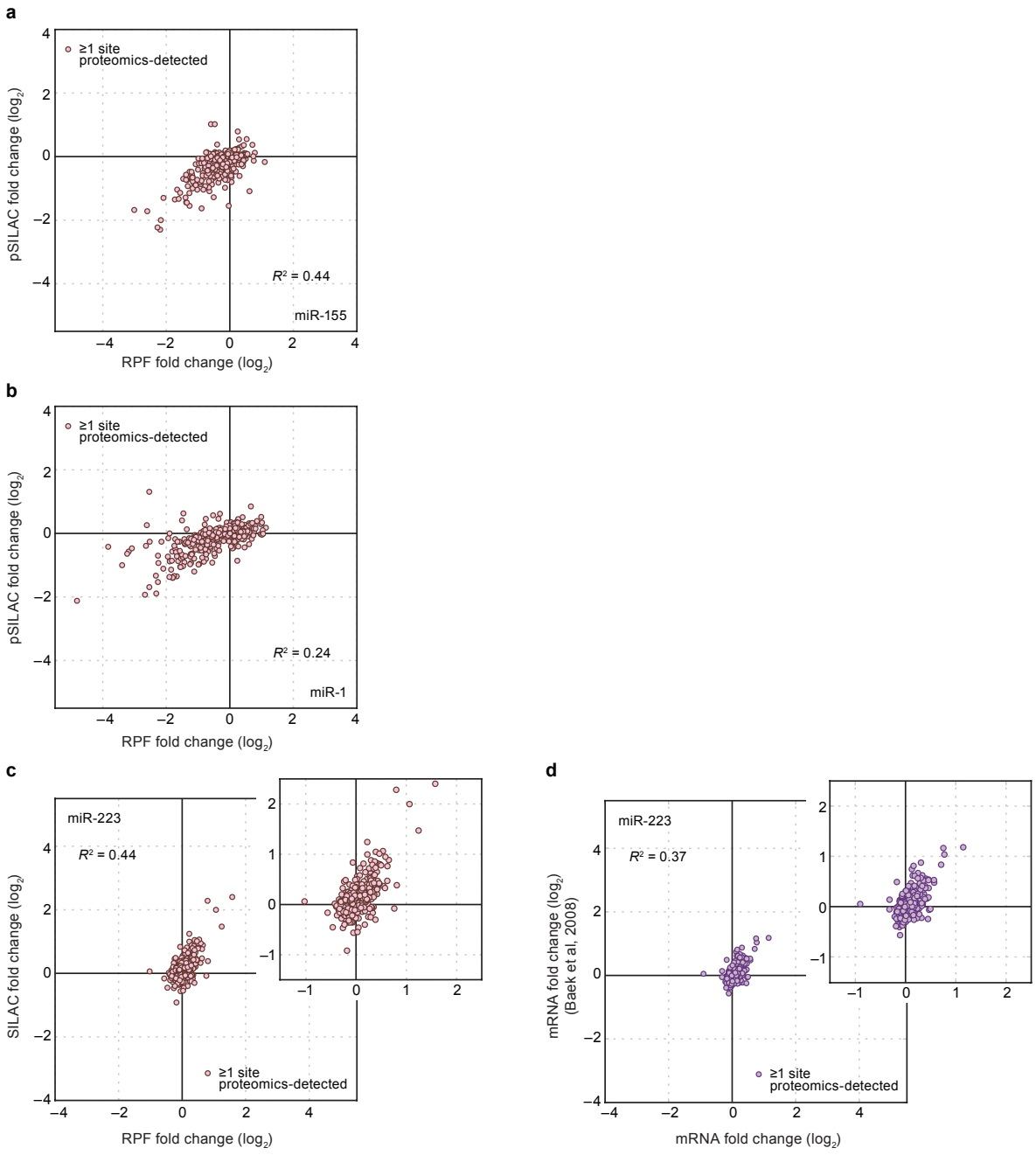

Supplementary Figure 11. Correspondence between ribosome changes, as measured by ribosome profiling, and changes in protein output, as measured by previous proteomics experiments. **a**, Correspondence between ribosome (RPF) and protein changes after introducing miR-155, plotting data for the 299 genes that had at least one miR-155 3'UTR site and were detected in the pSILAC experiment (proteomics-detected). The R^2 derived from Pearson's correlation is indicated. **b**, Correspondence between ribosome and protein changes after introducing miR-1, plotting data for the 386 genes that had at least one miR-1 3'UTR site and were detected in the pSILAC experiment. Otherwise, as in panel **a**. **c**, Correspondence between ribosome and protein changes after deleting *mir-223*, plotting data for the 337 genes that had at least one miR-223 3'UTR site and were detected in the SILAC experiment. Otherwise, as in panel **a**. The inset provides a closer view of the same data. **d**, Correspondence between mRNA changes in the Baek et al. (2008) experiment and the mRNA changes in the current experiment. Both axes plot fold changes measured on mRNA arrays for the 310 genes that 1) had at least one miR-223 3'UTR site, 2) were detected in the SILAC experiment, and 3) were assigned the identical transcript isoform in the two experiments.

In the experiments that ectopically introduced miRNAs, the ribosome changes tended to be larger than the protein changes (panels **a** and **b**). This difference might reflect different efficiencies of the miRNA transfections, which were performed in different labs. Alternatively, the difference might reflect a quantification caveat that arises when quantifying proteins that have accumulated under pre-steady-state conditions. Although the pSILAC experiment only quantified proteins synthesized after miRNA transfection, there still might have been a lag time before the impact of the transfected miRNA was fully exerted. Because pSILAC measured differences integrated over the time period of metabolic labeling, the maximal repression might have been underestimated if this lag time was substantial. The use of normal SILAC or direct-labeling methods for these and other pre-steady-state conditions would underestimate the maximal repression even more than would pSILAC. In contrast, ribosome profiling measures differences at one moment in time and thus is not subject to this quantification caveat. Consistent with this explanation, the protein changes tended to be at least as strong

as the ribosome changes in the miR-223 experiments (panel **c**), in which the cells that expressed miR-223 had been expressing this miRNA over many cell divisions, whereas those that had no miR-223 had never had this miRNA. Indeed, the changes appeared even greater in the previous experiment measuring protein changes compared to the current experiment measuring RPF changes (panel **c**). The simplest explanation for these differences is that the two biological samples differed, such that the miR-223 effects were greater when the experiment was done to collect the protein data compared to when the experiment was done to collect the RPF data (perhaps because in the first experiment samples were collected after eight days of differentiation, whereas in the second experiment samples were collected after only six days). Results from mRNA array data that had been collected on both biological samples, which showed greater mRNA differences in the first compared to the second experiment, supported this explanation (panel **d**). Therefore, the greater protein differences observed in panel **c** were due to greater effects in the first biological sample and were not evidence that the RPF changes failed to capture an aspect of miRNA regulation observed with the protein changes.

Taken together, the results of this figure indicate that changes observed by proteomics are no greater than those observed by ribosome profiling. Therefore, miRNAs do not change protein output or protein accumulation in a manner that might be missed by ribosome profiling, e.g., by co-translational degradation of nascent polypeptides, or by a reduction in the rate of translation initiation coupled with a correspondingly slower rate of elongation.